A Theoretical Study of a Novel Single-Electron Refrigerator Fabricated from Semiconductor Materials

A Theoretical Study of a Novel Single-Electron Refrigerator Fabricated from Semiconductor Materials

Hiroya Ikeda* and Faiz Salleh

Research Institute of Electronics, Shizuoka University, Hamamatsu 432-8011, Japan

We propose a novel single-electron refrigerator (SER) that can be fabricated from semiconductor materials such as a silicon-on-insulator wafer. The SER consists of a single-electron box and a single-electron pump (SEP). An equivalent circuit of the SEP refrigerator was derived. Its stability diagram (Coulomb diamond) was theoretically calculated and found to have a distorted honeycomb structure. In addition, a Monte Carlo simulation based on the orthodox theory for the Coulomb blockade phenomenon predicts successful single-electron extraction and injection.

1. Introduction

Single-electron devices utilizing the Coulomb blockade (CB) phenomenon are expected to realize ultra-low-power devices and new functional devices. A single-electron refrigerator (SER) is an interesting single-electron device that refrigerates by extracting and injecting a single electron.[1–9] The SER reported in the literature consists of a normal-metal/insulator/superconductor tunnel junction based on a single-electron box[10] It refrigerates a metal dot by single-electron tunneling to and from the superconductor electrode under an ac bias. There are mainly two principal physical points in the refrigeration process. One point involves extracting electrons with energies above the Fermi energy from the metal dot and injecting electrons with energies below the Fermi energy into the dot. Repeated electron extraction and injection reduces the temperature of the electron gas in the metal dot. The other point is electron transport without scattering in the superconductor electrode. This is critical since extracted and injected electrons must not raise the phonon temperature in the vicinity of the metal dot.

In the present paper, we propose a SER that has a novel device structure. It employs a single-electron pump (SEP)[10–12] and the refrigerator can be fabricated from semiconductor materials. Using Si-based materials will enable the SER to be employed to cool devices such as CPUs and displays. A Monte Carlo simulation based on the Coulomb blockade phenomenon

*E-mail address: ikeda@rie.shizuoka.ac.jp

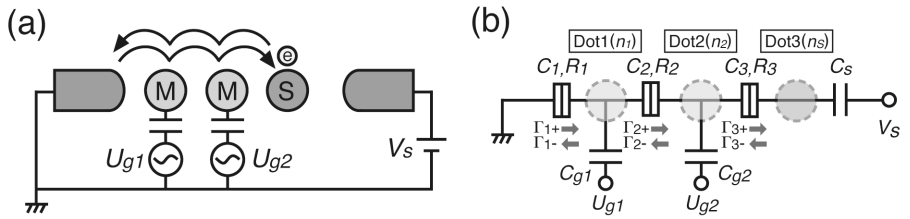

Fig. 1. (a) Schematic diagram of the SER device and (b) its equivalent circuit. M (dots 1 and 2) and S (dot 3) represent the metal and intrinsic semiconductor dots, respectively. n_i in parentheses is the number of extra electrons in the i-th dot. $\Gamma_{i\pm}$ indicates the electron-tunneling event to the right (or left) through the i-th junction.

demonstrates that the proposed SEP refrigerator can extract and inject individual electrons.

2. Structure and Principle of SEP Refrigerator

Figure 1(a) shows a schematic diagram of the SEP refrigerator, where M and S respectively represent metal and semiconductor dots. The left side of the device diagram corresponds to the SEP circuit. The two metal dots are connected to the source electrode and the semiconductor dot via tunnel junctions. Ac gate biases U_{g1} and U_{g2} can be individually applied to each metal dot via gate capacitances. Individual electrons can be transferred in the simple SEP circuit by applying ac biases with an appropriate phase difference. Moreover, the electron transfer direction can be selected independently of the drain bias.[10–12] The right side of Fig. 1(a) corresponds to the single-electron-box circuit. The semiconductor dot functions as an electron box and its electrostatic potential can be controlled by an external bias V_S via a control capacitor C_S. Hereafter, we refer to V_S as the control bias. We expected that, by applying suitable V_S biases, it would be possible to extract an electron from the conduction band in the semiconductor dot and to inject it into the valence band. Thus, the semiconductor dot is refrigerated by forcibly transferring an electron from the conduction band to the valence band.

We first theoretically discuss single-electron transfer in the equivalent circuit shown in Fig. 1(b). Boxes with center lines indicate tunnel junctions. The i-th tunnel junction has a capacitance C_i and a tunnel resistance R_i. Points surrounded by tunnel junctions and capacitors correspond to dots and are indicated by circles bounded by dashed lines. Dots 1 and 2 are metallic dots, and dot 3 is an intrinsic semiconductor dot. n_i in parentheses represents the number of extra electrons in the i-th dot, and $\Gamma_{i\pm}$ indicates electron tunneling to the right (positive sign) and the left (negative sign) through the i-th junction.

We analytically calculate the CB condition for this circuit and plot its stability diagram

in the (U_{g1}, U_{g2}) plane in the usual manner.[13,14] By considering the stored charge Q_i in the capacitor C_i, the free energy of the SEP-refrigerator circuit can be expressed as

$$F(n_1, n_2, n_S) = \frac{Q_1^2}{2C_1} + \frac{Q_2^2}{2C_2} + \frac{Q_3^2}{2C_3} + \frac{Q_S^2}{2C_S} + \frac{Q_{g1}^2}{2C_{g1}} + \frac{Q_{g2}^2}{2C_{g2}} - Q_S V_S - Q_{g1} U_{g1} - Q_{g2} U_{g2}, \quad (1)$$

where the Q_is satisfy the following equations:

$$V_S = \frac{Q_1}{C_1} + \frac{Q_2}{C_2} + \frac{Q_3}{C_3} + \frac{Q_S}{C_S},$$

$$U_{g1} = \frac{Q_1}{C_1} + \frac{Q_{g1}}{C_{g2}}, \quad U_{g2} = \frac{Q_1}{C_1} + \frac{Q_2}{C_2} + \frac{Q_{g2}}{C_{g2}},$$

$$Q_1 - Q_2 - Q_{g1} = -en_1, \quad Q_2 - Q_3 - Q_{g2} = -en_2, \quad Q_3 - Q_S = -en_S.$$

We then calculate the change in the free energy $\Delta F^{\pm} = F(n_i \pm 1) - F(n_i)$ for an electron-tunneling event $\Gamma_{i\pm}$. The CB condition can be obtained from $\Delta F^{\pm} > 0$. Figure 2 shows the obtained stability diagram for $C_1 = C_2 = 5$ aF, $C_3 = 3.75$ aF, $C_{g1} = C_{g2} = 1.3$ aF, $C_S = 50$ aF, and $V_S = 0$ V. In this calculation, C_3 was taken to be smaller than C_1 and C_2. The band diagram for V_S biasing for electron extraction and injection indicates that a tunneling electron must travel through both the semiconductor dot and the capacitor C_3. Therefore, the semiconductor dot should be represented in the equivalent circuit as a capacitor in series. The index $(n_1 n_2; n_S)$ in Fig. 2 corresponds to the numbers of extra electrons in dots 1, 2, and 3. The six lines are the boundaries for the CB condition for $\Gamma_{i\pm}$ tunneling under the (00;0) configuration. The hexagonal domain bounded by the six boundary lines is referred to as the Coulomb diamond; no electrons can tunnel at 0 K in this domain because of the CB condition, and thus the circuit is stable in this domain.

As is well known, the CB domain is characterized by the index $(n_1 n_2; n_S)$. The shaded regions in Fig. 2 indicate the domains for the $(01; -1)$ and $(10; -1)$ configurations. They have hexagonal shapes and the stability diagram has a honeycomb pattern that is similar to that of a simple SEP circuit.[10,11] Therefore, an electron can be transferred from the semiconductor dot to the source electrode when two periodic signals having the same frequency but with a phase difference of $\pi/2$ are applied to make a clockwise circle around the triple point shared by domains (00;0), $(01; -1)$, and $(10; -1)$ in the stability diagram shown in Fig. 2.

The hexagon bounded by a dashed line near the origin is the CB domain characterized by the $(00; -1)$ configuration. The domain $(00; -1)$ is slightly distorted compared with the domain (00;0). This indicates that the extra electron (extra hole when $n_S = -1$) in the semiconductor dot modifies the CB condition in the SEP region, as reported in our previous study for a circuit that does not contain any semiconductor dots (i.e., a three metal-dot

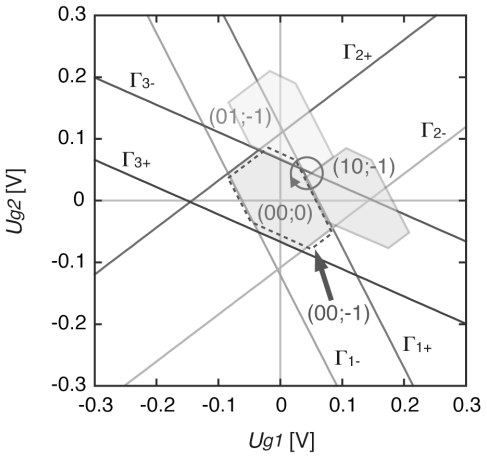

Fig. 2. Stability diagram for the SEP-refrigerator circuit for $C_1 = C_2 = 5$ aF, $C_3 = 3.75$ aF, $C_{g1} = C_{g2} = 1.3$ aF, $C_S = 50$ aF, and $V_S = 0$ V. The index $(n_1 n_2; n_S)$ corresponds to the numbers of extra electrons in dots 1, 2, and 3. The six lines are the boundaries for the CB condition for $\Gamma_{i\pm}$ tunneling in the case of (00;0).

system).[15,16]

Figure 2 reveals that SEP operation requires three sides shared by each two Coulomb diamonds. To realize SEP operation for a given control bias, it is desirable for the Coulomb diamond to have long sides (i.e., for the diamond to have a large area). For this purpose, we evaluate the U_{g2} intercepts of the CB-condition boundaries for Γ_{1+}, Γ_{2+}, and Γ_{3-} when $(00;0)$ under $V_S = 0$ V:

$$U^0_{g2}(\Gamma_{1+}) = e\frac{C_{g2}C_S + C_2(C_3 + C_S) + C_3(C_{g2} + C_S)}{2C_2C_{g2}(C_3 + C_S)}, \tag{2}$$

$$U^0_{g2}(\Gamma_{2+}) = e\frac{(C_{g1} + C_{g2})C_S + C_1(C_3 + C_S) + C_3(C_{g1} + C_{g2} + C_S)}{2(C_1 + C_{g1})C_{g2}(C_3 + C_S)}, \tag{3}$$

$$U^0_{g2}(\Gamma_{3-}) = e\frac{C_{g1}(C_{g2} + C_S) + C_1(C_2 + C_{g2} + C_S) + C_2(C_{g1} + C_{g2} + C_S)}{2(C_1 + C_2 + C_{g1})C_{g2}C_S}. \tag{4}$$

Figure 3 shows the U_{g2} intercepts for Γ_{1+}, Γ_{2+}, and Γ_{3-} tunneling calculated using Eqs. 2 to 4 as functions of the control capacitance C_S and the gate capacitance for the condition $C_{g1} = C_{g2}$. The other capacitances are set to $C_1 = C_2 =$10 aF and $C_3 =$5 aF. Figure 3(a) shows that the control capacitance C_S strongly influences the CB condition when C_S is comparable to the junction capacitance C_i. For $C_S <$20 aF, $U^0_{g2}(\Gamma_{1+})$ and $U^0_{g2}(\Gamma_{2+})$ decrease, and $U^0_{g2}(\Gamma_{3-})$ increases sharply with decreasing C_S. The Coulomb diamond is not hexagonal when $U^0_{g2}(\Gamma_{3-})$ is larger than $U^0_{g2}(\Gamma_{1+})$ and $U^0_{g2}(\Gamma_{2+})$ (see Fig. 2), which indicates that SEP operation will not occur under this condition. On the other hand, the CB condition is affected little by the control capacitance when $C_S \gg C_i$. Figure 3(b) reveals that all the U_{g2} intercepts increase sharply

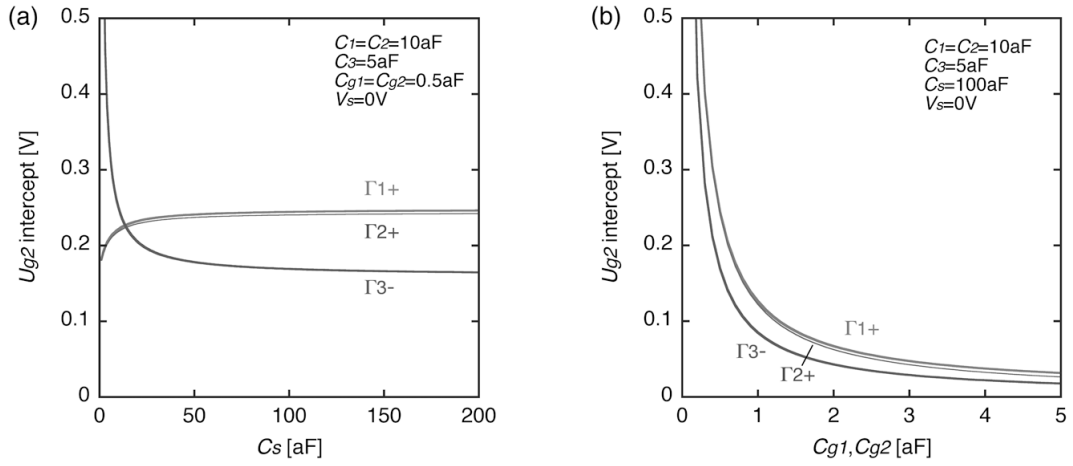

Fig. 3. U_{g2} intercepts for the CB condition for Γ_{1+}, Γ_{2+}, and Γ_{3-} tunneling as a function of (a) control capacitance C_S and (b) gate capacitance C_{gi} ($C_{g1} = C_{g2}$). The other circuit parameters are set to $C_1 = C_2$ =10 aF, C_3 =5 aF, and V_S =0 V.

with decreasing gate capacitance. Since the CB condition is determined by the charges, the voltage increases as the capacitance decreases, which is consistent with the result in Fig. 3(b). Hence, the gate capacitance C_{gi} should be as small as possible to maximize the area of the Coulomb diamond.

3. Monte Carlo Simulation of SET Operation

In this section, SET operation is estimated when the semiconductor dot is biased. Based on the results in Fig. 3, the circuit parameters are set to $C_1 = C_2 = 5$ aF, $C_3 = 2$ aF, $R_1 = R_2 = 1$ MΩ, $R_3 = 2$ MΩ, $C_{g1} = C_{g2} = 0.5$ aF, and $C_S = 100$ aF. Figure 4 shows the calculated stability diagrams for $V_S = 5$ and -5 mV. The six boundary lines in Figs. 4(a) and (b) are for $(00; 0)$ and $(00; -1)$, respectively. In Fig. 4(a), the Coulomb diamonds are almost pentagonal, and there is an aperture surrounded by three Coulomb diamonds. An aperture is also visible in Fig. 4(b), although the Coulomb diamonds are hexagonal. However, in both cases, there are three sides shared by each two domains in the stability diagram, and thus SEP operation is possible.

To clarify the transfer of individual electrons, the ac characteristics are calculated numerically using a Monte Carlo simulation[17] based on the orthodox theory of the CB phenomenon.[13,14] For simplicity, we ignore cotunneling effects in this calculation and set the operation temperature to 0 K, as we did in previous studies.[15,16,18–20] Details of the simula-

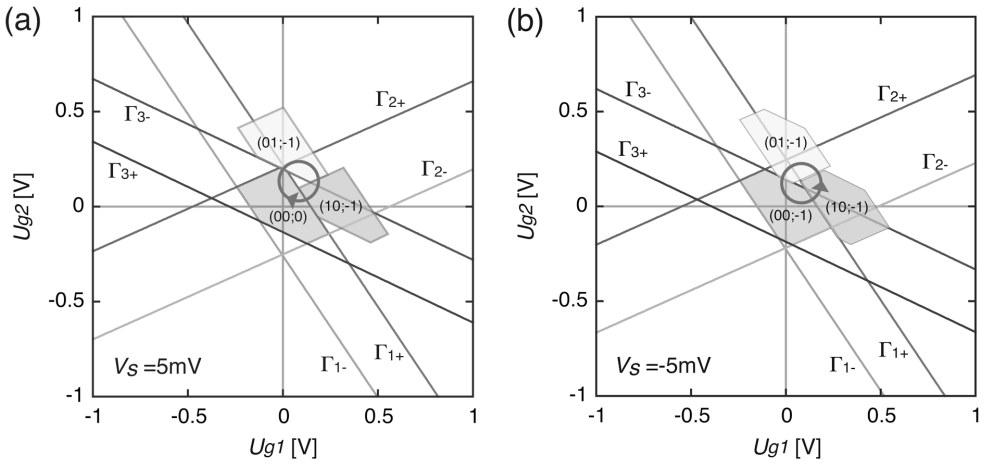

Fig. 4. Stability diagram of the SEP-refrigerator circuit for $C_1 = C_2 =$ 5 aF, $C_3 =$ 2 aF, $C_{g1} = C_{g2} =$ 0.5 aF, and $C_S =$ 100 aF. The control bias is (a) $V_S =$ 5 mV for electron extraction and (b) $V_S =$ -5 mV for electron injection. The six boundary lines in (a) and (b) are for (00;0) and (00;-1), respectively.

tion procedure are described in those studies. The electron movement in the dots is examined by applying 10 periods of a circular gate bias that consists of a series of clockwise and counterclockwise biases with periods of 200 μs. The control bias V_S is set to positive and negative during clockwise and counterclockwise biases, respectively.

Figure 5 shows typical changes in the numbers of extra electrons in the three dots (n_1, n_2, and n_S) for one period of the gate bias simulated at 0 K. The circuit parameters are $C_1 = C_2 =$5 aF, $C_3 =$2 aF, $R_1 = R_2 =$1 MΩ, $R_3 =$2 MΩ, $C_{g1} = C_{g2} =$0.5 aF, and $C_S =$100 aF. The control bias is $V_S = \pm$5 mV. At 28 μs, n_2 increases to 1 and n_S becomes -1. This indicates that electrons tunnel from the semiconductor dot to the central metal dot via junction 3 (Γ_{3-} tunneling event). A Γ_{2-} tunneling event then occurs at 65 μs and a Γ_{1-} tunneling event occurs at 86 μs. Consequently, in the first half of the gate bias, an electron is transferred from the semiconductor dot to the source electrode under $V_S = +5$ mV. Similarly, in the second half, an electron moves from the source electrode to the semiconductor dot under $V_S = -5$ mV. Therefore, a series of single-electron extractions and injections is realized under this condition.

The success rate of single-electron extraction and injection for 10 periods is evaluated by averaging 10 trial calculations at 0 K; it is plotted in Fig. 6 as a function of the absolute control bias $|V_S|$. Except for V_S, the circuit parameters are the same as those for Fig. 5. This figure clearly shows that the success rate is unity when $|V_S| < 5.6$ mV. However, at $|V_S| = 5.7$ mV, the success rate drops dramatically to 0.2, and it reaches zero at 6 mV. This is because the Coulomb diamond is almost triangular and the sides shared by the Coulomb diamonds

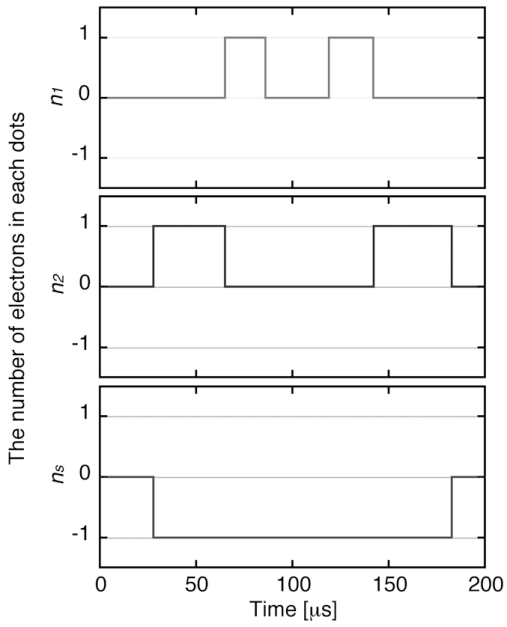

Fig. 5. Typical changes in the number of extra electrons in the dots n_1, n_2, and n_S for one period of the gate voltage simulated at 0 K. The circuit parameters are $C_1 = C_2$ =5 aF, C_3 =2 aF, $R_1 = R_2$ =1 MΩ, R_3 =2 MΩ, $C_{g1} = C_{g2}$ =0.5 aF, and C_S =100 aF. The control bias is $V_S = \pm 5$ mV.

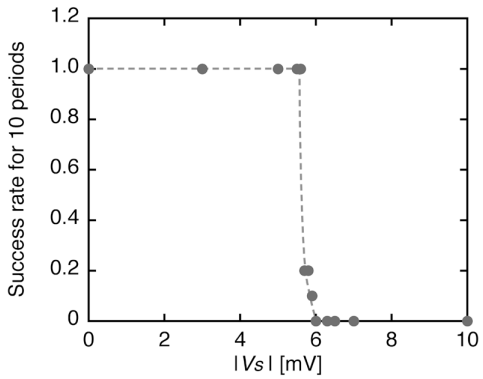

Fig. 6. Success rate of single-electron extraction and injection for 10 periods, averaged from 10 trial calculations at 0 K, as a function of absolute control bias $|V_S|$. The circuit parameters are the same as those in Fig. 5.

vanish when $|V_S| > 6$ mV.

The values of the tunnel capacitances (C_i) and the gate capacitances (C_{gi}) used in Fig. 2 were roughly estimated for Si dots in SiO_2 environment, in which the dot was a cubic 30 nm on a side and the distance between the dots was 5 nm. The gate-oxide thickness was

assumed to be 20 nm. According to the result of Fig. 3(a), C_S should be much larger than C_i. Therefore, we have to design the control-bias electrode whose area is effectively enough large since it is difficult to fabricate the distance between the semiconductor dot and the electrode to be below 5 nm. In addition, Fig. 6 indicates that the SEP refrigerator operates successfully only below $|V_S| = 5.6$ mV. This value is too small in comparison with the Si bandgap width. The further optimization of the circuit parameters will be necessary for the use of practical semiconductor materials.

4. Conclusions

We investigated SET operation for the equivalent circuit of a novel SER device that uses a SEP and is fabricated from semiconductor materials. The stability diagram of the equivalent circuit had a distorted honeycomb Coulomb diamond for a given control bias. Monte Carlo simulation revealed single-electron extraction and injection is possible by applying an appropriate circular bias at an operating temperature of 0 K. SEP operation could be realized at an absolute control bias below $|V_S| = 5.6$ mV.

References

1) M. Nahum, T. M. Eiles and J. M. Martinis: Appl. Phys. Lett. **65** (1994) 3123.
2) A. Bardas and D. Averin: Phys. Rev. B **52** (1995) 12873.
3) M. M. Leivo, J. P. Pekola and D. V. Averin: Appl. Phys. Lett. **68** (1996) 1996.
4) H.-O. Müller and K. A. Chao: J. Appl. Phys. **82** (1997) 453.
5) A. Luukanen, M. M. Leivo, J. K. Suoknuuti, A. J. Manninen and J. P. Pekola: J. Low Temp. Phys. **120** (2000) 281.
6) J. P. Pekola, T. T. Heikkilä, A. M. Savin, J. T. Flyktman, F. Giazotto and F. W. J. Hekking: Phys. Rev. Lett. **92** (2004) 056804.
7) A. M. Clark, N. A. Miller, A. Williams, S. T. Ruggiero, G. C. Hilton, L. R. Vale, J. A. Beall, K. D. Irwin and J. N. Ullom: Appl. Phys. Lett. **86** (2005) 173508.
8) F. Giazotto, T. T. Heikkilä, A. Luukanen, A. M. Savin and J. P. Pekola: Rev. Mod. Phys. **78** (2006) 217.
9) J. P. Pekola, F. Giazotto and O.-P. Saira: Phys. Rev. Lett. **98** (2007) 037201.
10) D. Esteve: in *Single Charge Tunneling, Coulomb Blockade Phenomena in Nanostructure*, ed. H. Grabert and M. H. Devoret (Plenum Press, New York, 1992) , p. 109.
11) H. Pothier, P. Lafarge, P. F. Orfila, C. Urbina, D. Esteve and M. H. Devoret: Physica B **169** (1991) 573.
12) M. W. Keller, J. M. Martinis, N. M. Zimmerman and A. H. Steinbach: Appl. Phys. Lett. **69** (1996) 1804.
13) K. K. Likharev: IEEE Trans. Magn. **23** (1987) 1142.
14) J. R. Tucker: J. Appl. Phys. **72** (1992) 4399.
15) H. Ikeda and F. Salleh: IEICE Tech. Rep. (ED2010-20, CPM2010-10, SDM2010-20) (2010) p. 17 [in Japanese].
16) H. Ikeda and F. Salleh: submitted to Adv. Mater. Res.
17) M. Kirihara, N. Kuwamura, K. Taniguchi and C. Hamaguchi: Ext. Abstr. Solid State Devices and Materials, 1994, p. 328.
18) M. Tabe, N. Asahi, Y. Amemiya, and Y. Terao: Jpn. J. Appl. Phys. **36** (1997) 4176.
19) M. Tabe, Y. Terao, R. Nuryadi, Y. Ishikawa, N. Asahi, and Y. Amemiya: Jpn. J. Appl. Phys. **38** (1999) 593.
20) H. Ikeda and M. Tabe: J. Appl. Phys. **99** (2006) 073705.